Talanta 134 (2015) 305–309

Contents lists available at ScienceDirect

Talanta

journal homepage: www.elsevier.com/locate/talanta

Sandwich-type electrochemical immunosensor using dumbbell-like nanoparticles for the determination of gastric cancer biomarker CA72-4

Dan Wu, Zhankui Guo, Yixin Liu, Aiping Guo, Wanruo Lou, Dawei Fan, Qin Wei *

Key Laboratory of Chemical Sensing & Analysis in Universities of Shandong, School of Chemistry and Chemical Engineering, University of Jinan, Jinan 250022, China

ARTICLE INFO

Article history:
Received 9 August 2014
Received in revised form
31 October 2014
Accepted 13 November 2014
Available online 20 November 2014

Keywords:
Reduced graphene oxide-tetraethylene pentamine (rGO-TEPA)
Gastric cancer biomarker CA72-4
PtPd-Fe_3O_4 nanoparticles
Immunosensor

ABSTRACT

A novel and sensitive nonenzymatic sandwich-type electrochemical immunosensor for the detection of gastric cancer biomarker CA72-4 was fabricated using dumbbell-like PtPd-Fe_3O_4 nanoparticles (NPs) as a novel kind of label. The signal amplification strategy, using the synergetic effect present in PtPd-Fe_3O_4 to increase the reduction ability of the NPs toward H_2O_2, improved the sensitivity of the immunosensor. The immunosensor was constructed by modifying glassy carbon electrode with reduced graphene oxide-tetraethylene pentamine (rGO-TEPA) for effective immobilization of primary anti-CA72-4 antibody (Ab_1). Secondary anti-CA72-4 antibody (Ab_2) was adsorbed onto the PtPd-Fe_3O_4 NPs. The proposed immunosensor displayed a wide linear range (0.001–10 U/mL) with the low detection limit (0.0003 U/mL). The immunosensor was evaluated for serum samples, receiving satisfactory results. Therefore, the immunosensor possesses excellent clinical value in cancer screening as well as convenient point-of-care diagnostics.

1. Introduction

Tumor markers are useful tools in the diagnosis of tumors, therefore the reliable and sensitive detection of tumor markers is currently the subject of intensive studies. Gastric cancer remains the second leading cause of cancer-related deaths worldwide. Carcinoembryonic antigen (CEA) and carbohydrate antigen 19-9 (CA19-9), commonly used in gastric cancer, have a limited clinical utility, due to their low sensitivity and specificity. One of the newer markers, tumor-associated glycoprotein TAG-72, also called cancer antigen 72-4 (CA72-4), seems to exhibit better characteristics compared with the other two markers [1]. CA72-4 is a mucin with high molecular weight (220–400 kDa). It is identified by using monoclonal antibody B72-3. CA72-4 has been widely used to diagnose cancer and to monitor immunotherapy. Its reported specificity (92%) and positive predictive value (86%) are high [2]. Preoperative levels of this tumoral marker may aid in predicting the invasiveness of gastric cancer and in providing prognostic information for patients. Thus, it has significance for the early detection of the gastric cancer related with biomarker CA72-4. Sandwich-type immunosensors give the highest level of sensitivity and specificity because of the use of a couple of match antibodies. Therefore, sandwich-type assay is one of the most popular schemes in the immunosensings and immunoassays [3–6]. In this article, we developed a convenient sandwich-type immunosensor for the sensitive detection of CA72-4. The immobilization of antibody is important for the increase of sensitivity of the immunosensor. Reduced graphene oxide (rGO) has attracted great attention in the fabrication of immunosensors because of their excellent chemical and electrical properties [7–10]. Meanwhile, rGO may also be functionalized through covalent or non-covalent methods in order to further enhance its sensitivity, specificity, loading capacity, biocompatibility, etcetera. Reduced graphene oxide-tetraethylene pentamine (rGO-TEPA) is a novel material which is combined by rGO and tetraethylene pentamine through covalent bond. It not only keeps the original property of rGO but also promotes the water solubility. In addition, rGO-TEPA has large number of amino groups which can form covalent bonds with other materials to enhance the performance of rGO-TEPA easily. Thus, in order to enhance the sensitivity of the sensor, rGO-TEPA was introduced to immobilize primary antibody (Ab_1) during the modification of electrochemical sensor.

Among various NPs reported, Pt and its alloy NPs showed much enhanced catalytic activity for H_2O_2 reduction reaction with the H_2O_2 detection limit reaching 2 μmol/L level [11, 12]. Dumbbell-like NPs have shown some interesting catalytic properties due to the interfacial interactions between two different nanostructures. For example, dumbbell-like Au – Fe_3O_4 and Pt – Fe_3O_4 were found to be more active than either single component for H_2O_2 reduction in PBS [13]. The enhanced activity is believed to come from the

* Corresponding author. Tel.: +86 531 82765730; fax: +86 531 82765969.
E-mail address: sdjndxwq@163.com (Q. Wei).

http://dx.doi.org/10.1016/j.talanta.2014.11.025
0039-9140/

partial charge transfer between Au (or Pt) and Fe_3O_4 at the nanoscale interface. Due to the intrinsic high activity of Pt-based alloys and dumbbell-like NPs, the PtPd – Fe_3O_4 NPs should have even higher activity for the reduction reaction and therefore have higher sensitivity for H_2O_2 detection [14, 15].

For sandwich-type immunosensors, the signal is mainly determined by the use of the label. Various nanoparticle labels including noble metal nanoparticles, carbon nanomaterials, semiconductor nanoparticles, metal oxide nanostructures, and hybrid nanostructures, have been developed [16–19]. To the best of our knowledge, there is no report focusing on electrochemical detection of CA72-4 based on dumbbell-like PtPd-Fe_3O_4 nanoparticles as label. In continuation of our previous works, the dumbbell-like PtPd-Fe_3O_4 NPs were prepared and indeed showed synergetic effect in catalyzing H_2O_2 reduction, which is more active than PtPd or Fe_3O_4 alone. With the secondary antibody (Ab_2) adsorbed onto PtPd, the resulting PtPd-Fe_3O_4-Ab_2 was used as label for the preparation of immunosensor to detect CA72-4. The sandwich-type structure is formed by immobilizing the primary CA72-4 antibody (Ab_1) onto rGO-TEPA through an amidation reaction between the amine groups attached to rGO-TEPA and the available carboxylic acid of Ab_1. The enhanced sensitivity was achieved due to the large surface area of rGO-TEPA for Ab_1 loading, high conductivity of rGO-TEPA for promoting the electron transfer, high catalytic activity of dumbbell-like PtPd-Fe_3O_4 NPs for accelerating the reduction of H_2O_2. Therefore, this simple, economic and sensitive immunosensing approach displayed promising application in clinic screening and diagnostics.

2. Experimental section

2.1. Materials and reagents

Reduced graphene oxide-tetraethylene pentamine (rGO-TEPA) was purchased from Nanjing XFNANO Materials TECH Co., Ltd. (China). CA72-4 and corresponding antibody were purchased from Shanghai Linc-Bio Science Co. Ltd. (China). Oleylamine (OAm) and 1-octadecene (ODE) were purchased from Aladdin. Oleic acid (OA), $K_3[Fe(CN)_6]$ and hexane were purchased from Sinopharm Chemical Reagent Co., Ltd.. Bovine serum albumin (BSA, 96–99%) was purchased from Sigma (USA) and used as received. 1-ethyl-3-(3dimethylamino-propyl) carbodiimide (EDC) and N-hydroxysuccinimide (NHS) were obtained from the Sinopharm Chemical Reagent Co., Ltd (China). Phosphate buffered saline (PBS, 0.1 mol/L containing 0.1 mol/L NaCl, pH 7.0) was used as an electrolyte for all electrochemistry measurement. Doubly distilled water was used throughout the experiments.

2.2. Apparatus

All electrochemical measurements were performed on a CHI 760D electrochemical workstation (Shanghai CH Instruments Co., China). Electrochemical impedance spectroscopy (EIS) was obtained from the impedance measurement unit (IM6e, ZAHNER elektrik, Germany). Transmission electron microscope (TEM) images were obtained from a Hitachi H-800 microscope (Japan). High resolution TEM (HR-TEM) observations were performed on a JEOL-2100 with an accelerating voltage of 200 kV.

2.3. Preparation of dumbbell-like PtPd-Fe_3O_4 nanoparticles

Dumbbell-like PtPd-Fe_3O_4 nanoparticles were synthesized according to the Ref. [15]. The typical procedure is shown in Supporting Information. For comparison, PtPd and Fe_3O_4 nanoparticles were synthesized according to the Ref. [20] and Ref. [21], respectively.

2.4. Preparation of PtPd-Fe_3O_4-Ab_2 label

The as synthesized PtPd-Fe_3O_4 NPs (1 mg) were dispersed in 1.0 mL of cetyltrimethylammonium bromide (CTAB, 0.02 g) solution. The mixture was stirred for 0.5 h and then centrifuged. After discarding the supernatant, the mixture was dispersed in 1 mL of phosphate buffer. Then, 10 μg/mL secondary antibody (Ab_2) was added into the solution and the mixture was allowed to react at room temperature under stirring for 24 h, followed by centrifugation. Ab_2 could be immobilized on PtPd-Fe_3O_4 nanoparticles through adsorption and it has been proved that amino groups in CA72-4 Ab_2 can be bound strongly to Pt (or Pd) [22]. The resulting PtPd-Fe_3O_4-Ab_2 was washed with pH 7.0 PBS and then redispersed in buffer and stored at 4 °C before use.

2.5. Modification of electrodes

Primary antibodies were immobilized onto the surface of rGO-TEPA through an amidation reaction between the amine groups attached to rGO-TEPA and the available carboxylic acid of Ab_1. Typically, the solution containing EDC (50 mmol/L) and NHS (50 mmol/L) was added into 1 mL rGO-TEPA (2 mg/mL) solution. The mixture was stirred for 4 h. Then 1 mL of Ab_1 solution (10 μg/mL) was added to the above solution. After another 4 h of reaction with stirring, the mixture was centrifuged. The resulting rGO-TEPA-Ab_1 conjugates were re-dispersed in PBS and stored at 4 °C before use.

Fig. 1 showed the fabrication procedure of the immunosensors. A glassy carbon electrode with 3-mm diameter was polished to a mirror-like surface with 1.0, 0.3 and 0.05 μm alumina powder and then thoroughly cleaned before use. Firstly, 6.0μL of rGO-TEPA-Ab_1 solution was coated on the working electrode and then dried. The electrode was then thoroughly rinsed with PBS. After that the electrode was incubated in 1 wt% bovine serum albumin (BSA) solution for another 30 min to eliminate nonspecific binding sites. Subsequently, CA72-4 solution with varying concentrations was added to the electrode surface and incubated for 1 h at 4 °C, and then the electrode was washed extensively to remove unbound CA72-4 molecules. Finally, the prepared PtPd-Fe_3O_4-Ab_2 solution was dropped onto the electrode surface and incubated for another 1 h. The amount of label captured was in accordance with the CA72-4 concentration due to the specific antibody-antigen interaction. After washing, the prepared electrode was stored at 4 °C prior to use.

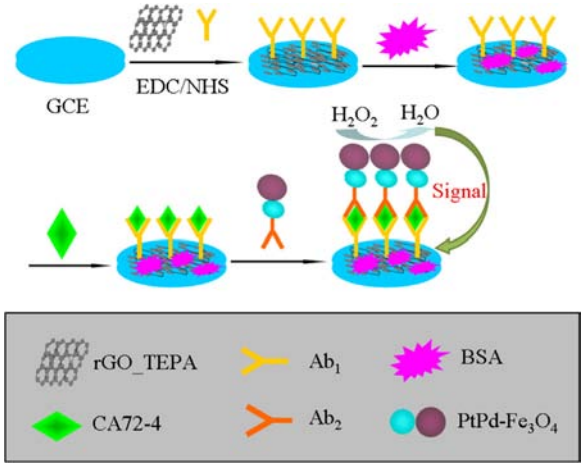

Fig. 1. Fabrication steps of the immunosensor.

2.6. Characterization of the immunosensor

A conventional three-electrode system was used for all electrochemical measurements: a glassy carbon electrode as the working electrode, a saturated calomel electrode (SCE) electrode as the reference electrode, and a platinum wire electrode as the counter electrode. pH 7.0 PBS was used for all the electrochemical measurements. Cyclic voltametry (CV) was recorded in PBS at 100 mV/s. For amperometric measurement of the immunosensor, −0.4 V was selected as detection potential because such a low potential would be beneficial to decrease the background current and minimize the responses of common interference species. After the background current was stabilized, 5.0 mmol/L H_2O_2 was added to the buffer solution, and the current change was recorded. The electrochemical impedance spectroscopy (EIS) was scanned in pH 7.0 PBS containing 2.5 mmol/L $K_3[Fe(CN)_6]$ and 0.1 mol/L KCl. All measurements were performed at room temperature.

3. Results and discussion

3.1. Characterization of rGO-TEPA and PtPd-Fe_3O_4 NPs

As shown in Figs. 2A and B, rGO-TEPA with a wrinkled paper-like structure was observed. It had the large surface area in favor of electron transportation. Meanwhile, rGO-TEPA, containing more amino groups, assisted its reaction with Ab_1 through an amidation reaction, thereby increasing the stability of the modified electrodes.

In this study, the dumbbell-like PtPd-Fe_3O_4 NPs were used to label anti-CA72-4 Ab_2 due to their high sensitivity toward H_2O_2 reduction. The TEM image of the PtPd-Fe_3O_4 NPs is shown in Fig. 2C. The darker regions correspond to PtPd NPs because PtPd has a higher electron density than that of Fe_3O_4. The as-synthesized PtPd-Fe_3O_4 heterostructures have dumbbell-like structures.

3.2. Characterization of PtPd-Fe_3O_4 NPs modified electrode

The electrochemical responses of the developed immunosensors toward H_2O_2 were further investigated. To understand the sensitivity of the developed immunosensors on H_2O_2 reduction by NPs, 6 μL of PtPd, Fe_3O_4, and PtPd-Fe_3O_4 NPs solution (2 mg/mL) was coated onto the electrodes surface to prepare the corresponding modified electrode, respectively. After dried, the corresponding modified electrode was obtained. After the addition of the same concentration of H_2O_2, the largest reduction current was observed with the PtPd-Fe_3O_4 modified electrode, as shown in Fig. 3C. The reduction current of the Pt-Fe_3O_4 electrode is even higher than the reduction current of the PtPd (Fig. 3A) and Fe_3O_4 (Fig. 3B) electrodes together, indicating that the synergetic effect is present in the PtPd-Fe_3O_4 NPs. This synergetic effect on the immunosenor was already proved in dumbbell-like Au-Fe_3O_4 NPs [23, 24].

3.3. The electrochemical characterization of the modified electrode

EIS was used to characterize the interface properties of the modification of the electrode [25, 26]. The impedance spectra include a semicircle portion and linear portion. The semicircle diameter at higher frequencies corresponds to the electron-transfer resistance, and the linear part at lower frequencies corresponds to the diffusion process [27]. The semicircle diameter equals the electron-transfer resistance (R_{ct}). Fig. 4 shows the Nyquist diagrams of electrochemical impedance spectra. It is easy to see that the EIS of rGO-TEPA modified electrode (curve b) is similar to that of the bare GCE (curve a). The reason may be that rGO-TEPA is an excellent electrically conducting material, which makes electron transfer easier. After incubation with Ab_1, Rct increased which indicates Ab_1 was immobilized on the electrode successfully and blocked electron transfer (curve c). And an obvious increase in R_{ct} was observed after BSA was immobilized on the surface of Ab_1/rGO-TEPA/GCE, resulting from hindering the diffusion of $[Fe(CN)_6]^{4-/3-}$ toward the electrode surface by BSA (curve d). Subsequently, R_{ct} increased again (curve e), which indicates the successful capture of CA 72-4 and the formation of immunocomplex layer blocking the electron transfer. When PtPd-Fe_3O_4-Ab_2 nanoparticles were immobilized, R_{ct} increased to the maximum (curve f), which indicates that the electrode was well-modified.

3.4. Optimization of experimental conditions

Current change was mainly due to the interaction between the label of PtPd-Fe_3O_4 and the substrate of H_2O_2. Since the high sensitivity of PtPd-Fe_3O_4-Ab_2 for H_2O_2 detection, immunosensors using PtPd-Fe_3O_4-Ab_2 as labels were built and characterized. A relatively high amount of Ab_2 was attached onto the PtPd-Fe_3O_4 surface. Thus, when CA72-4 was present on the electrode, then PtPd-Fe_3O_4-Ab_2 labels could be easily captured onto the electrode surface through the specific antibody-antigen interaction and the amount of label captured is in accordance with CA72-4 concentration. So the immunosensor can be used for quantitative determination CA72-4 concentration.

The analytical performance of the immunosensor was related to the pH value of the detection solution. The acidity of the solution greatly affected the activity of the immobilized protein and the sensitivity of the electrochemical immunosensors. The effect of pH on the CV peak current was tested over a pH range from 6.0 to 9.0 at constant concentrations of CA72-4. As shown in Fig. 5, it was found that the peak current increased with increasing pH value from 6.0 to 7.0 to reach the maximum and decreased from pH 7.0 to 9.0. Thus, the optimal amperometric response is achieved at pH 7.0. The reason is that the highly acidic or alkaline surroundings would damage the immobilized protein [28]. So pH 7.0 PBS was selected for the test throughout this study. The concentration of rGO-TEPA was also important factors that affected the performance of the immunosensor. It was found that

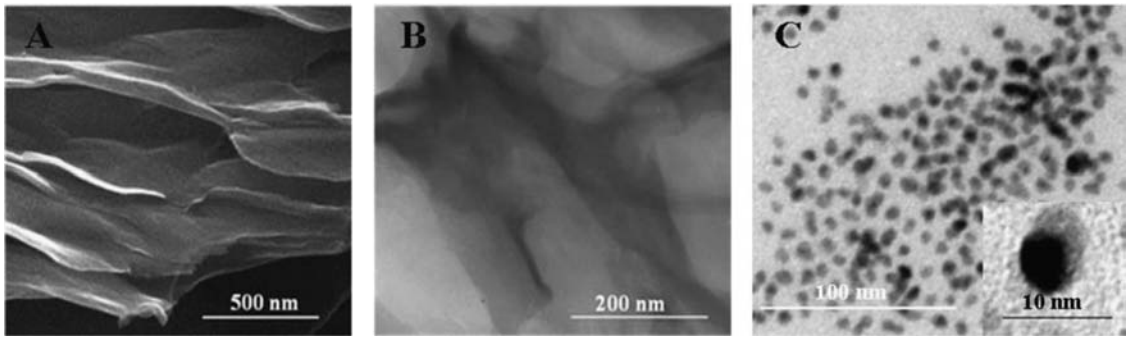

Fig. 2. SEM image of rGO-TEPA (A), TEM images of rGO-TEPA (B) and PtPd-Fe_3O_4 (C).

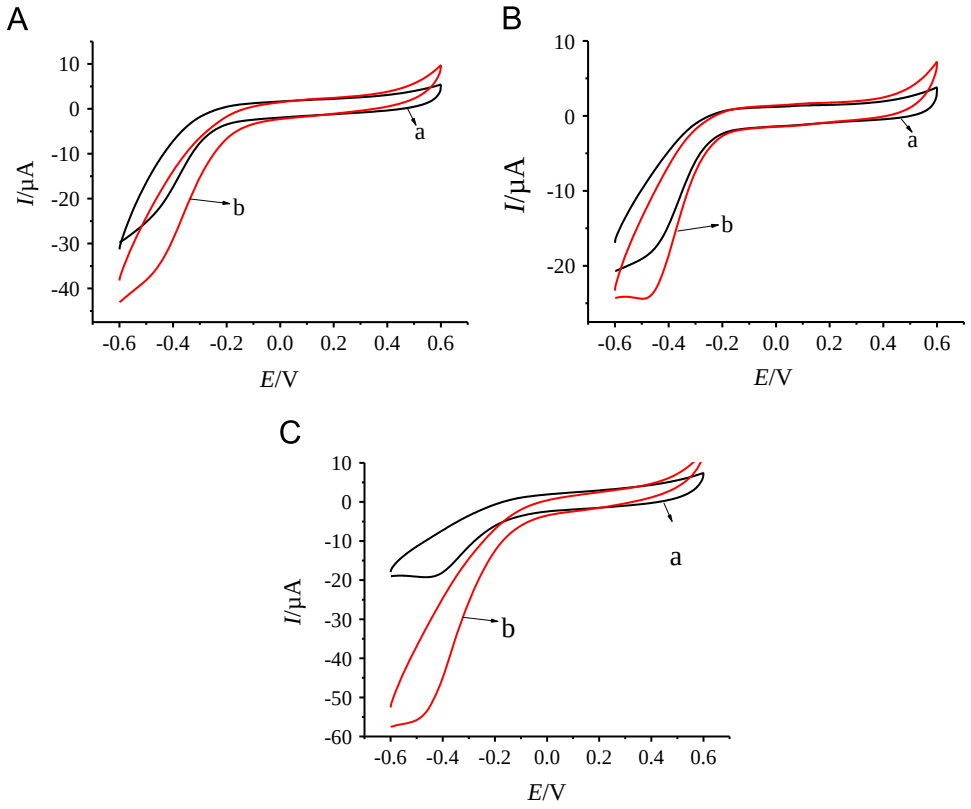

Fig. 3. Cyclic voltammograms of (A) PtPd, (B) Fe_3O_4 and (C) PtPd -Fe_3O_4 modified electrode in PBS (pH=7.0) without (a, black) and with (b, red) 5 mmol/L H_2O_2.

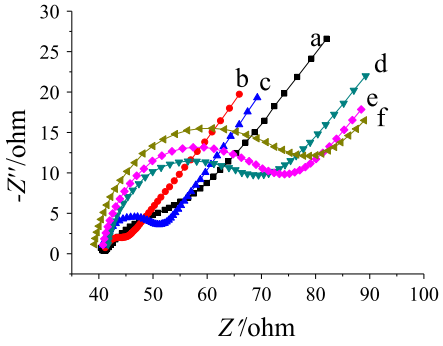

Fig. 4. Nyqiust plots of the electrochemical impedance spectroscopy (EIS) for each immobilized step in 2.5 mmol/L $[Fe(CN)_6]^{4-/3-}$ – 0.1 mol/L KCl solution. The bare GCE (a), rGO-TEPA/GCE (b), Ab_1/rGO-TEPA/GCE (c), BSA/Ab_1/rGO-TEPA/GCE (d), CA72-4/BSA/Ab_1/rGO-TEPA/GCE (e), and Ab_2/CA72-4/BSA/Ab_1/rGO-TEPA/GCE (f).

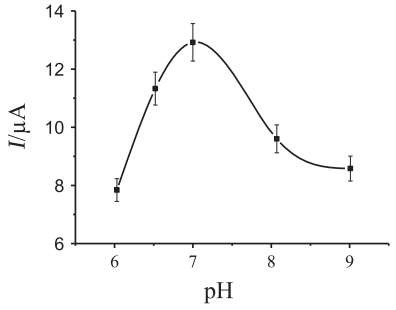

Fig. 5. Effect of pH on the response of the immunosensor to 10 U/mL CA72-4.

the best concentration of rGO-TEPA was 2.0 mg/mL because the current reached the maximum value.

Since the high sensitivity of the immunosensor using PtPd-Fe_3O_4-Ab_2 as label has proved, a series of immunosensors was prepared for the detection of different concentration of CA72-4. The current response increased with the increasing of CA72-4 concentration in the range from 0.001 to 10 U/mL, with a detection limit of 0.0003 U/mL based on S/N=3. Compared with the detection limit for time-resolved immunofluorometric assays (TR-IFMA) (0.55 U/mL) [2] and electrochemical immunosensors (0.10 U/mL) [29], the proposed immunosensor has lower detection limit. The reasons why the immunosensor has the low detection limit were as follows: firstly, rGO-TEPA could greatly increase the loading of Ab_1 due to its high surface area and more amino; secondly, as discussed earlier, the high catalytic activity of PtPd-Fe_3O_4-Ab_2 toward H_2O_2 increased the sensitivity of the immunosensor; and lastly, the good conductivity and electrons transfer ability of rGO-TEPA could also help the detection of H_2O_2 and lower the detection limit.

3.5. Reproducibility, selectivity, and stability

To evaluate the reproducibility of the immunosensors, a series of five electrodes were prepared for the detection of 2 U/mL CA72-4. The amperometric responses were 6.00 μA, 5.92 μA, 5.60 μA, 5.32 μA, 5.60 μA, respectively and the relative standard deviation (RSD) of the measurements for the five electrodes was 4.8%, suggesting that the reproducibility of the proposed immunosensor was quite good.

The selectivity of the immunosensor was also tested. 2 U/mL of CA72-4 solution containing different interfering substances was measured by the immunosensor. For BSA and SCCA interfering substances, the concentrations were 100 ng/mL, respectively. For CA12-5 and CA19-9 interfering substances, the concentrations were 200 U/mL, respectively. It can be seen from the result that the current variation due to the interfering substances was less than 2.1% of that without interferences, indicating that the interferences of relatively high concentrations only had negligible effects on CA72-4 detection, and the selectivity of the proposed immunosensor was acceptable.

Table 1
Results for the determination of CA72-4 in the serum sample.

Sample	Content in sample (U/mL, $n=5$)	Added (U/mL)	Found (U/mL, $n=5$)	RSD (%, $n=5$)	Recovery (%, $n=5$)
Serum 1	1.82	5.00	6.74	4.2	98.4
Serum 2	1.25	5.00	6.43	3.5	104

The storage stability of the immunosensor was also examined by storing one electrode in pH 7.0 PBS at 4 °C when not in use, and at the different storage periods the immunosensor is used to detect the same concentration of CA72-4. The results indicate the immuosensor retained 99.7% of its initial response after 5 days storage and its response decreased to 92.6% after 10 days.

3.6. Real sample analysis

The amount of CA72-4 in human serum sample was measured 5 times and the relative standard deviation (RSD) was calculated to obtain the precision. The accuracy was also studied through a recovery experiment using standard addition method. An appropriate amount of CA72-4 standard solution was added to corresponding samples. The experiments were also repeated five times. The recovery, referring to the average recovery, was calculated to obtain the accuracy. It can be seen from Table 1 that the relative standard deviation was in the range of 3.5%–4.2% and the recovery was between 98.4%–104%. Thus, the proposed method could be satisfactorily applied to the clinical determination of CA72-4 in human serum.

4. Conclusions

Using CA72-4 as a model of tumor marker for gastric gancer, the immunosensor could be prepared by immobilizing the capture antibodies onto reduced graphene oxide-tetraethylene pentamine through an amidation reaction. The large surface area of reduced graphene oxide-tetraethylene pentamine increases the amount of Ab_1 immobilized onto electrode surface. The synergetic effect present in PtPd-Fe_3O_4 enhances the reduction ability of NPs toward H_2O_2 and it was used for the efficient labels. This developed immunosensor showed high sensitivity, good selectivity and reproducibility, and acceptable stability, providing a promising approach for clinical research and diagnostic applications.

Acknowledgments

This study was supported by the Natural Science Foundation of China (No. 21405059, 21103071 and 21377046). Qin Wei thanks the Special Foundation for Taishan Scholar Professorship of Shandong Province and University of Jinan.

Appendix A. Supporting information

Supplementary data associated with this article can be found in the online version at http://dx.doi.org/10.1016/j.talanta.2014.11.025.

References

[1] D. Marrelli, E. Pinto, A.D. Stefano, M. Farnetani, L. Garosi, F. Roviello, Am. J. Surg. 181 (2001) 16–19.
[2] S.L. Sheng, Q. Wang, G. Huang, Clin. Chim. Acta 380 (2007) 106–111.
[3] X. Pei, B. Zhang, J. Tang, B. Liu, W. Lai, D. Tang, Anal. Chim. Acta 758 (2013) 1–18.
[4] M. Yang, H. Li, A. Javadi, S. Gong, Biomaterials 31 (2010) 3281–3286.
[5] R. Cui, J.J. Zhu, Electrochim. Acta 55 (2010) 7814–7817.
[6] Y. Fu, P. Li, T. Wang, L. Bu, Q. Xie, X. Xu, L. Lei, C. Zou, J. Chen, S. Yao, Biosens. Bioelectron. 25 (2010) 1699–1704.
[7] X. Jia, Z. Liu, N. Liu, Z. Ma., Biosens. Bioelectron. 53 (2014) 160–166.
[8] B. Sun, L. Chen, Y. Xu, M. Liu, H. Yin, S. Ai, Biosens. Bioelectron. 51 (2014) 164–169.
[9] S.K. Mishra, A.K. Srivastava, D. Kumar, A.M. Biradar, Rajesh, Nanoscale 5 (2013) 10494–10503.
[10] A.J. Haque, H. Park, D. Sung, S. Jon, S.Y. Choi, K. Kim, Anal. Chem. 84 (2012) 1871–1878.
[11] B.D. Adams, C.K. Ostrom, A.J. Chen, Electrochem. Soc 158 (2011) B434–B439.
[12] R.D. O'Neil, S. Chang, J.P. Lowry, C.J. McNeil, Biosens. Bioelectron. 19 (2004) 1521–1528.
[13] Y. Lee, M.A. Garcia, N.A.F. Huls, S. Sun, Angew. Chem., Int. Ed. 49 (2010) 1271–1274.
[14] X. Sun, S. Guo, C.S. Chung, W. Zhu, S. Sun, Adv. Mater. 25 (2013) 132–136.
[15] X. Sun, S. Guo, Y. Liu, S. Sun, Nano Lett. 12 (2012) 4859–4863.
[16] Y. Liu, M. Chi, V. Mazumder, K.L. More, S. Soled, J.D. Henao, S. Sun, Chem. Mater. 23 (2011) 4199–4203.
[17] S. Sun, H. Zeng, D.B. Robinson, S. Raoux, P.M. Rice, S.X. Wang, G. Li, J. Am. Chem. Soc. 126 (2004) 273–279.
[18] J. Qian, C. Zhang, X. Cao, S. Liu, Anal. Chem. 82 (2010) 6422–6429.
[19] G. Wang, X. Gang, X. Zhou, G. Zhang, H. Huang, X. Zhang, L. Wang, Talanta 103 (2013) 75–80.
[20] Y. An, X. Jiang, W. Bi, H. Chen, L. Jin, S. Zhang, C. Wang, W. Zhang, Biosens. Bioelectron. 32 (2012) 224–230.
[21] H. Wang, D. Sun, Z. Tan, W. Gong, L Wang, Colloid Surf. B 84 (2011) 515–519.
[22] S. Mandal, D. Roy, R.V. Chaudhari, M. Sastry, Chem. Mater. 16 (2004) 3714–3724.
[23] Q. Wei, Z. Xiang, J. He, G. Wang, H. Li, Z. Qian, M. Yang, Biosens. Bioelectron. 26 (2010) 627–631.
[24] G.K. Parshetti, F. Lin, R. Doong, Sens. Actuator B 186 (2013) 34–43.
[25] W.J. Jin, G.J. Yang, H.X. Shao, A.J. Qi, Sens. Actuator B 188 (2013) 271–279.
[26] H. Huang, P. Ran, Z. Liu, Bioelectrochemistry 70 (2007) 257–262.
[27] H.J. Chen, Z.H. Zhang, R. Cai, X. Chen, Y.N. Liu, W. Rao, S.Z. Yao, Talanta 115 (2013) 222–227.
[28] R. Yuan, D.P. Tang, Y.Q. Chai, X. Zhong, Y. Liu, J.Y. Dai, Langmuir 20 (2004) 7240–7245.
[29] H. Fan, Z. Guo, L. Gao, Y. Zhang, D. Fan, G. Ji, B. Du, Q. Wei, Biosens Bioelectron 64 (2015) 51–56.